Desalination and Water Treatment
www.deswater.com
doi: 10.1080/19443994.2016.1165737

57 (2016) 25939–25949
November

Taylor & Francis
Taylor & Francis Group

Development of monopolar and platinum intermediate bipolar membranes: application in desalting brine solution

Krishnaveni Venugopal, Sangeetha Dharmalingam*

Department of Mechanical Engineering, Anna University, Guindy, Chennai 600025, Tamil Nadu, India, Tel. +91 044 22357763; Fax: +91 044 22357744; emails: rvveni@gmail.com (K. Venugopal), sangeetha@annauniv.edu (S. Dharmalingam)

Received 14 September 2015; Accepted 17 February 2016

ABSTRACT

The desalination process parameters like current efficiency (CE), energy consumption, and acid–base production for the fabricated bipolar membrane (BPM) electrodialysis unit (five compartments of 120 cm^2 active areas) were investigated in this paper using monopolar- and bipolar-based ion-exchange membranes (IEMs). Also, the performance of the fabricated unit in removing NaCl was assessed in terms of salinity. Polystyrene–ethylene–butylene–polystyrene was functionalized to prepare the monopolar and bipolar IEMs. In the case of BPM, platinum was used as the intermediate layer. The synthesized IEMs were characterized thermally and by contact angle measurements. A commercially procured monopolar and bipolar ion-exchange membrane made of polystyrene–divinylbenzene was also evaluated for the purpose of comparison. The electrodialysis process using these IEMs reached the highest CE of 66 and 38% with the lowest energy consumption of 0.24 Wh and 1.60 Wh for the synthesized and commercial membrane, respectively.

Keywords: Brine solution; Bipolar membrane; Platinum; Salinity measurement; Water splitting

1. Introduction

Water is the elixir of life. Next to oxygen, water is the most important substance essential for sustaining human life. Water resource in general, can be divided into conventional and non-conventional sources and is distributed throughout the world in different forms. But in India, there are many villages and towns which do not have adequate and reliable sources of drinking water of required qualities. Thus, governments focused their attention toward effective use of existing resources or to find an alternative source for drinking water from other water bodies such as brackish water, sea water, and sewage water using suitable techniques like desalination in order to restrict water demands.

Desalination is used worldwide as a reliable source of fresh water supply since seawater is principally an unlimited source. Desalinated water is often the last resort for many countries to overcome water shortages and it can also be used for watering municipal gardens, agricultural fields, and for certain industrial processes. The maintenance cost of the installed desalination plants was expected to be relatively expensive since it uses multi-compartment membrane-based electrodialysis (ED) technique [1] which has been seen historically as a very energy intensive process.

---

*Corresponding author.

During the past 25 years a lot of work has been done in the field of ion-exchange membranes (IEMs) for their applications in industrial effluents treatment and desalination of sea and brackish water. In general, IEM can be either monopolar or bipolar in nature. The advantage of the ED process over reverse osmosis is the elimination of secondary salt pollution by recovering the ions in the form of acid and base solutions along with the salt removed from the feed solution by making use of monopolar and bipolar ion-exchange membranes [2,3]. Bipolar membrane electrodialysis (BPMED)-based desalination technique is nothing but a combination of conventional ED and water dissociation feature due to the presence of catalytic intermediate layer (IL) in a bipolar membrane (BPM).

The presence of heterogeneous materials like ion-exchange resin (IER) particles in a non-conducting polymer matrix of an IEM [4] along with the catalytic intermediates like weak acid such as phenolic, carboxylic acid, or phosphoric acid groups [5] and its corresponding base, inorganic substances such as Mg, Ni, Co, Mn, Cu, Fe, and Al [6], metallic compounds such as ruthenium trichloride, chromic nitrate, indium sulfate, and hydrated zirconium oxide, [7,8], heavy/noble metal ions like Cr^{3+}, Fe^{2+}, Ag, Au, Pt, Pd, Os, Rh, Ti, Sn, Zr, Pa, and Ru [9,10], macromolecules such as polyethylene glycol [11], polyvinyl alcohol [12], and bovine serum albumin containing both carboxylic and amino groups [13], and starburst dendrimer polyamidoamine [14] in between the cation-exchange layer (CEL) and anion-exchange layer (AEL) of BPM as IL; usually results in BPM with higher mechanical stability [15] with improved water dissociation effects when compared with the BPM prepared using lamination of CEL and AEL alone without any IL.

In the present work, we have prepared monopolar (cation exchange (CEM) and anion exchange (AEM)) and bipolar (with platinum (Pt) as IL) IEMs with resin and glass fiber reinforcements using polystyrene–ethylene–butylene–polystyrene (PSEBS) polymer. The prepared IEMs were characterized using TGA, contact angle, and some laboratory techniques. The water dissociation capacity of the prepared BPM with Pt intermediate was tested in a two-compartment electrodialytic cell. The membranes were evaluated for their desalination efficiency on diluted real sample brine solution of approximately 10,000 ppm up to 8 h. The stack performance using the synthesized membranes was compared with that of the commercial polystyrene–divinylbenzene-based (PSDVB) IEMs under similar experimental conditions. In addition, the decrease in salinity of the feed water was also observed.

2. Experimental methodology

2.1. Required materials

Chlorosulfonic acid, tributyl phosphate, and paraformaldehyde were obtained from Lancaster and Central Drug House (CDH), respectively. Triethyl amine, chloroform, conc. HCl, and NaOH were obtained from Spectrochem. Tetrahydrofuran (THF) and methanol were purchased from Merck. Commercial strong acid cation-exchange membrane (CMI–7000S) and commercial strong base anion-exchange membrane (AMI–7001S) were procured from Membranes International INC, New Jersey, USA. While, BPM made up of PSDVB represented as BPM-II were procured from Arun Electro chemicals, Chennai. Glass fiber was purchased from Meena glass fiber industry. Seralite (Cation-Exchange resin (CER)— equivalent to Amberlite IRC–120, 20–50 mesh standard grade), Seralite (Anionic-exchange resin (AER)—equivalent to Amberlite IRA–400, 20–50 mesh standard grade), and zinc chloride were obtained from Sisco Research Laboratory Pvt. Ltd, (SRL). Platinum chloride (Pt) and poly(styrene–ethylene–butylene–polystyrene triblock copolymer (PSEBS) ($M_w = 89{,}000$, $M_w/M_n < 1.06$) was purchased from Aldrich (USA).

2.2. Preparation of reinforced IEMs

Cationic and anionic functionalized ionomers or sulfonated polystyrene–ethylene–butylene–polystyrene (SPSEBS) and quaternized polystyrene–ethylene–butylene–polystyrene (QPSEBS) ionomers were obtained as per the procedure explained in the S1 section of supporting information [16]. To enhance the ion-exchange capacity (IEC), firmness, and strength of the non-reinforced membranes, it was reinforced with resin and glass fiber. Reinforced cationic exchange membrane (RCEM) or reinforced sulfonated polystyrene–ethylene–butylene–polystyrene (RSPSEBS) and reinforced anionic exchange membrane (RAEM) or reinforced quaternized polystyrene–ethylene–butylene–polystyrene (RQPSEBS) based on PSEBS polymer was prepared by first dispersing a specific quantity (from 10 to 70%) of dried (60˚C for 24 h in an oven) and crushed CER/AER in either SPSEBS/QPSEBS-THF solution for 12 h using magnetic stirrer at room temperature. In order to break the aggregates and to obtain a uniform dispersion, the solution was sonicated for 30 min. Then, the solution was cast on a clean glass petridish and the glass fiber matrix was placed to get immersed in the solution before drying in the oven for 24 h at 45˚C.

The obtained membranes with various resin content were subjected to conductivity studies as described in the supporting information S2 and from Table S1, it was observed that the conductivity of the prepared membranes increased with increase in IER loadings below 50%, beyond which the membranes became brittle. Hence, the resin loading was optimized at 40% for both resins [17]. Reinforced bipolar membrane (RBPM, i.e. RPSEBS-Pt) was prepared using RCEM (RSPSEBS) and RAEM (RQPSEBS) as CEL and AEL, respectively. The AEL and CEL layers were cut into pieces of 10 × 12 cm size, pretreated using 1 M NaOH and 1 M HCl solutions, then finally equilibrated with 2 M NaCl solution, washed with distilled water and dried. Then, on one side of both CEL and AEL layers, a platinum chloride solution containing approximately 6 mL of 0.12 g of Pt was coated to form the IL. Finally, the IL-coated side of both layers (CEL and AEL) were sandwiched and subjected to hot press for 5 min at a temperature and pressure of about 64˚C and 3 ton, respectively, to finally obtain RBPM-Pt represented as RPSEBS-Pt-based IEM system or simply BPM-I system.

2.3. Characterization of reinforced IEMs

The incorporation of resin into functionalized PSEBS membrane was confirmed with Perkin Elmer RX I FTIR spectrophotometer and the discussion about the obtained spectra has been already reported in [18]. The thermal stability of the prepared membranes was studied using SDT Q 600 US analyzer (ASTM E1131) under a nitrogen atmosphere with a heating rate of 20˚C/min from room temperature to 700˚C. The average contact angle “θ” of 3 μL distilled water droplet obtained using a motor-driven syringe on the surface of polymers which was attached to the glass slides using a double-sided adhesive tape was measured at RT and the hydrophilic and hydrophobic nature of the membranes was determined using Goniometer-sessile drop meter GBX-Digi-drop wetting and spreading studies. The conductivity of the membranes was determined using impedance spectroscopy as described in the supporting information S2. Water absorption and IEC for the prepared membranes were measured using the similar procedure as discussed earlier [19]. The chemical stability of membranes was analyzed by accelerating the degradation process using a solution containing 4 ppm of ammonium iron (II) sulfate hexahydrate and 15 ml of H_2O_2 (3%) (Fentons reagent) in 500 ml of distilled water at 60˚C for about an hour.

2.4. Construction and working of multi-compartment ED stack

The five-compartment BPMED unit (Fig. S1(b) of supporting information) used in the study for the determination of IEM performance toward brine desalination was supplied by Arun Electrochemical, Chennai. The same instrument was altered into two compartments setup for the determination of BPM efficiency (Fig. S1(a) of supporting information) [18]. The cathode and anode electrodes used were stainless steel and Ti coated with Ti–Ru–Pd oxides, respectively. The two electrodes were connected to a DC power supply. The active membrane area of each membrane and volume of each chamber was about 120 cm^2 and 160 cm^3, respectively. Each compartment was connected to a tank of 1-L capacity of the distilled water solution, allowing for batchwise recirculation mode operation of external solutions using submersible pumps. The configuration of the membrane arrangement in the multi-compartment ED stack is in the order BPM–AEM–CEM–BPM in between the electrodes. And the five compartments of the BPMED unit were EC–AC–FC–BC–EC (where, EC stands for electrolyte compartment placed at the two extremes, adjacent to the electrodes; FC stands for feed compartment where the sample to be treated was circulated; AC and BC stands for acid and base compartments, respectively, placed adjacent to the feed compartment on either side) as represented in Fig. S1(b) of supporting information.

In order to minimize the cell voltage generated during the initial stages of the performance, dilute HCl (0.01 N) and dilute NaOH (0.01 N) solutions were used in AC and BC, respectively. And, 0.05 Mol/L of NaCl solution was used in each EC. Because at lower concentrations, higher resistances between membranes resulted and at higher concentrations, the selective nature of the IEMs became lower. The experiments were carried out at the initial voltage of 10 V. During the performance, at every 15 min time interval, process parameters such as pH and acid–base concentration of the solutions in various compartments were determined using a pH meter (Hanna HI 96107 pocket-size pH meter) and standard acid–base titration procedure, respectively. In addition, other parameters such as energy consumption, current efficiency (CE), transport number (T. No.) of ions, water dissociation efficiency (WDE), and water dissociation fluxes were determined using the same set of equations as discussed in S3 section of supporting information [20,21]. After 8-h treatment, the feed sample was analyzed for their salinity using WTW LF 197-S EC meter.

3. Results and discussion

3.1. Thermogravimetric analysis

The TGA curves of the reinforced monopolar and BPMs are shown in Fig. 1. The reason for the various degradation steps observed at certain temperatures for the membranes such as pristine polymer (PSEBS), reinforced monopolar (RSPSEBS and RQPSEBS), and commercial BPM was already discussed in our earlier report [18]. In addition, the TGA curve of BPM-I (RBPM-Pt), as observed from Fig. 1(d), exhibited four stages of degradation. The first weight loss was observed up to 184℃ which was attributed to the removal of physically and chemically bonded water along with the trace amounts of solvent from the polymer matrix. The second loss observed beyond 260℃ was due to the removal of both sulfonic and quaternary ammonium functional groups from the polymer backbone. The third weight loss occurring at temperature between 316 and 395℃ may be due to the removal of an intermediate molecule along with loosely bound IER particles present on the surface and from the reinforced polymer matrix. The fourth weight loss which was observed beyond 430℃ represents the degradation of reinforced fiber along with polymer main chain from the matrix.

3.2. Contact angle measurement

From the contact angle values, it was identified that the introduction of functional group converts the pristine PSEBS polymer (84.39˚) into a hydrophilic polymer with a smaller contact angle as studied by Dias and de Pinho [22] and Guan et al. [23]. The contact angles of the commercial monopolar membranes such as CEM-PSDVB and AEM-PSDVB were measured to be 86.70˚–93.09˚, respectively. A contact angle value for the reinforced functioned membranes such as RSPSEBS and RQPSEBS could not be measured due to complete absorption of water. This infers that the increased hydrophilicity of these membranes than the pristine membrane was due to the presence of functional groups, resins, and fiber reinforcements [24]. In order to determine the nature of Pt intermediate in BPM, one face of the membrane was coated with Pt solution and its contact angle was measured and was found to be 57.64˚.

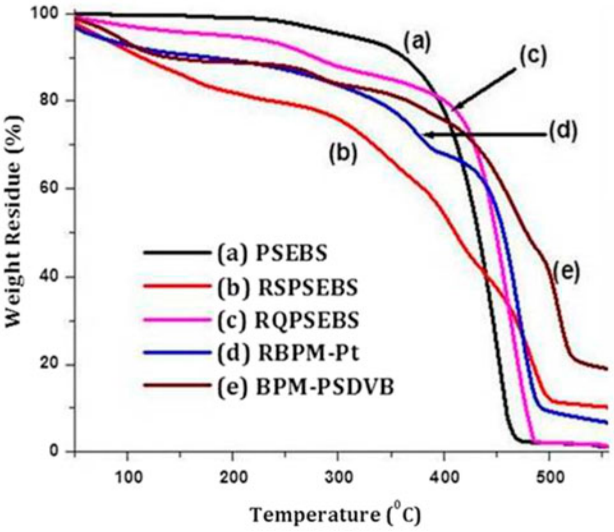

Fig. 1. TGA curves of (a) PSEBS, (b) RSPSEBS, (c) RQPSEBS, (d) RBPM-Pt, and (e) BPM-PSDVB.

3.3. Chemical stability

To determine the suitability of the prepared reinforced IEMs and commercial IEMs in BPMED unit, all the membranes was subjected to chemical stability test using Fenton's reagent. The generated peroxides attacked the polymer chains to undergo faster degradation. All the subjected samples were then checked for their water absorption, IEC, and conductivity values as per the standard procedures [19] and the discussion of the observed results were reported earlier [18]. While in the case of BPM-I, although the reinforced fibers held the IEMs strongly, due to the enhanced degrading mechanism, the incorporated hydrophilic resins and functional groups that were present on the surface leached out from the membranes due to loosening of the fibers upon swelling which resulted in lower water absorption (value of about 66% than its initial 88%) and conductivity values (value of about 5.1×10^{-3} S cm^{-1} from its initial 6.9×10^{-3} S cm^{-1}) [25].

3.4. Characterization of BPM-I and BPM-II

3.4.1. pH variation with time

Since BPM consisted of RCEM and RAEM as CEL and AEL layers, respectively, which were joined together using a catalytic Pt as IL, when it was placed in between the electrodes due to large electric field appearing at the membrane interface, an excess OH^- and H^+ ions were produced by the enhanced chemical reaction as discussed in detail in S4 section of the supporting information. This then migrated through the ion-exchange layers into the distilled water-filled compartments resulting in the formation of acid and base. This acid and base yields were analyzed using the change in pH measurements. From Fig. 2 it was obvious that with increase in time, the pH of the

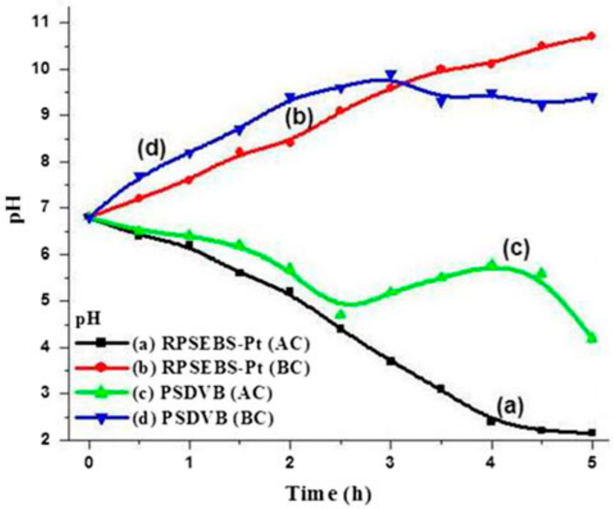

Fig. 2. Variation of pH with time in both acid and base compartments.

solutions in the two compartments changed from its initial distilled water value. The compartment closer to the anode side was found to be basic in nature and the one closer to the cathode side was acidic in nature. The increasing trend in pH change with time confirmed that some ions were produced newly during the performance due to certain *in situ* reactions. These ions probably were protons and hydroxyl ions and formed on either side of the BPM as a result of water splitting into its ions under the electrical driving force between the electrodes. This conclusion was arrived at ease as there was no possibility of any other ions formed since only distilled water was taken in both the compartments.

3.4.2. Concentration changes with time

The maximum concentration of 0.006 and 0.004 N was achieved as acid and base solutions in about an hour in the case of BPM-I when compared to BPM-II (beyond 2 h). In both BPMs, once the higher concentration was reached in both AC and BC; decrease in concentration was observed for BPM which exhibited a higher leakage and was observed to get leveled off without further rise or decrease if the leakage was not much favored in BPM. Hence, from the above discussion and from Fig. 3, it was confirmed that BPM-I showed a better performance than BPM-II.

3.5. BPMED stack performance for brine desalination

3.5.1. Determination of pH changes with time

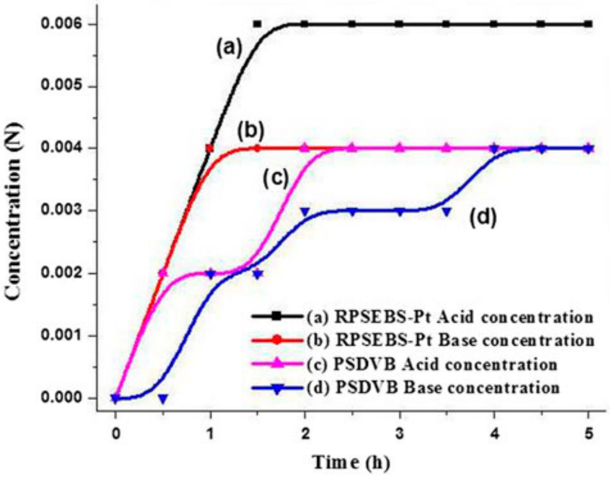

Fig. 3. Acid–base concentration in both AC and BC with time.

Fig. 4 represents the pH changes with time for both BPM-I and BPM-II systems. The pH of the solutions in FC, EC, AC, and BC was observed regularly at every 15 min interval up to 8 h. In the case of BPM-I system, the pH in FC was observed to decrease gradually and finally become acidic in nature [26]. This is because with increase in time, higher quantities of acid were produced due to water dissociated products and thereby resulting in proton leakage through IEMs depending upon the capacity of protons to

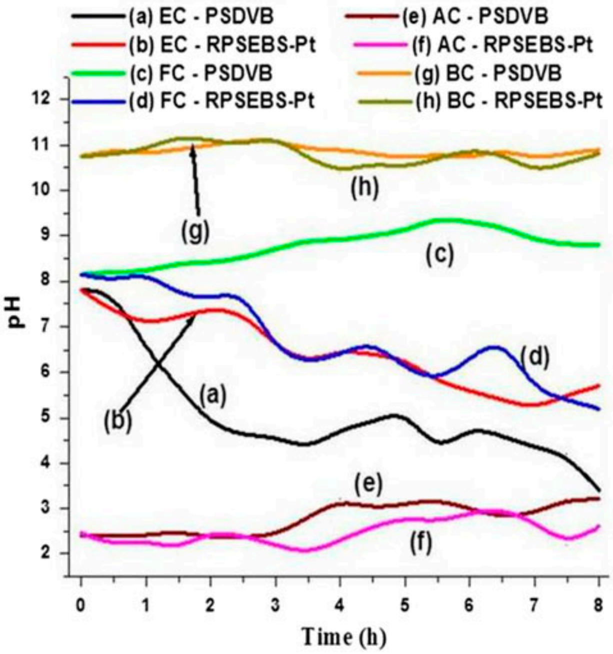

Fig. 4. Variation of pH in FC, EC, AC, and BC with time for the stack performance.

undergo back diffusion [27,28]. Due to its intrinsic mobility in the presence of water, FC remained acidic in nature. On the other hand, in the case of BPM-II system, the feed solution finally became basic in nature. The difference in pH observed between the two different systems was mainly attributed to the leakage of ions occurring through the membranes between the compartments in a stack. BPM-II based cell experienced a greater leakage of ions from BC to FC and thus it remained basic in nature. It was also reported that the proton leakage through BPM-II system was lower due to lower concentrations of acid that was produced during the BPMED process [26]. In the case of EC, due to the initial addition of 0.05 M NaCl solution, the pH was observed to be slightly basic during the initial stages, which was then observed to be decreasing with time. Though both the IEM systems showed the final solution to be acidic, the acidity was greater in the case of BPM-II system than that observed with BPM-I system. The reason for this was attributed to the higher leakage of ions through commercial membrane than the synthesized membrane.

From Fig. 4, it was clear that the initial pH in AC and BC was found to be in the range of ~2.45 and ~10.74, respectively, due to the addition of 0.01 N acid and 0.01 N base solutions into their respective compartments. Moreover, the pH in both AC and BC was found to rise marginally during the initial stage and was not uniform because of the leakage of certain ions into the neighboring compartments. Later, due to higher acid production, higher acidic pH and hence greater acid leakage were observed in the case of BPM-I system when compared to BPM-II system. Whereas, in the case of basic pH, both the systems showed more or less the same pH during the initial period of performance and later BPM-I system showed a little lower basic pH when compared to BPM-II system. Such a pH change in AC and BC confirmed the acid–base production in their respective compartments which can also be confirmed by their conductivity and concentration measurements. This pH variation in various compartments clearly suggested that both systems possessed adequate capacity to split water into its coions under electric fields.

3.5.2. Determination of acid and base concentrations

When the entire ED cell was under an electric field, the Na^+ and Cl^- ions were continuously transported from FC into BC and AC, respectively. In addition to this, an excess OH^- and H^+ ions produced at the AEL–CEL interface due to the field-enhanced chemical reaction (as discussed in S4 section of the supporting information) also permeated through the IELs resulting in the acid–base formation. From the pH studies, it was evident that acid and base of certain concentrations were produced in the AC and BC, respectively, for both the systems. From Fig. 5, it was noted that a maximum acid concentration of 0.012 and 0.008 N was achieved for BPM-I and BPM-II systems, respectively. Similarly, a maximum base concentration of 0.006 and 0.004 N was achieved for BPM-I and BPM-II systems, respectively.

The commercial BPM-II-based IEM cell was meant for base production rather than acid production because of higher specific permselectivity of CEM for H^+ ions as reported in the literature [26]. However, in our study, from Fig. 5, the alkalinity concentration was observed to be lower in case of BPM-II system. This can be more due to the higher intrinsic mobility of H^+ ions than the OH^- ions and hence resulting in higher leakage of H^+ ions. The T. No. of protons through AEM increased with acid concentration which would also lead to their lower concentration in AC. The maximum concentration remained constant until certain duration of time after which it decreased with increase in processing time for both types of IEM system. This suggested that the mass transfer of Na^+ and Cl^- ions through the IEM diminished due to the decrease in NaCl concentration in the feed solution. Together with the increase in the concentration of Na^+ and Cl^- ions in BC and AC, the molecular back diffusion through the IEM was caused by the high concentration gradient which might also hinder the transport of Na^+ and Cl^- ions. Furthermore, the dissociation of water molecules was also enhanced due to the second Wien effect.

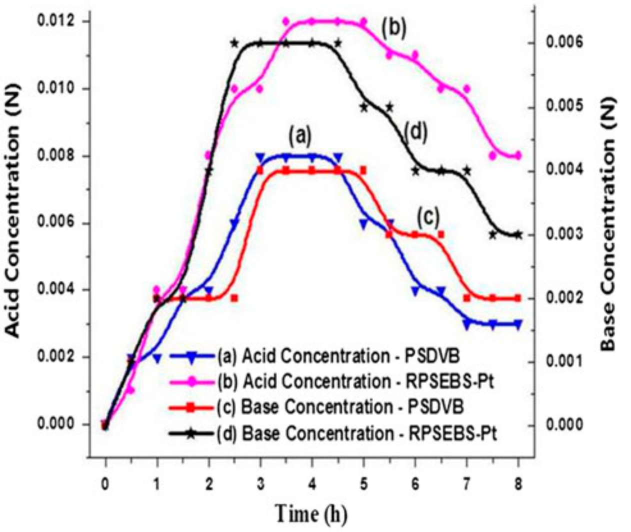

Fig. 5. Variation in acid and base concentrations with time for the stack performance.

3.5.3. Determination of T. No. of ions, WDE and its fluxes

The BPMED process efficiency is strongly affected by the transport properties of ions present in the solution and WDE. Under an electric field, at the beginning of the BPMED process, there was a competition between the ions such as Na^+, Cl^-, H^+, and OH^- for transport, and the transfer of a large amount of Na^+ and Cl^- ions through the IEM resulted in a slow transfer of H^+ and OH^- ions. This was because of the maximum availability of initial salt concentration in FC when compared with the water-dissociated ions. As the operation time passed, the dissociation of large amounts of water molecules resulted in the large accumulation of H^+ and OH^-. It should be noted that once all the Na^+ and Cl^- ions were transported from the FC, the accumulated H^+ and OH^- were also transported very efficiently resulting in the higher WDE after the first-half performance time. This also explained the reason for the observed higher T. No. of ions with time during the first-half part of the performance and a decrease in its value during the later stages of performance for the same membrane [26].

Ion T. No. indicates the contribution of ions toward acid–base production, depending upon its electrical mobility under electric current. Fig. 6 represents the T. No. properties of both sodium and chloride ions for BPM-I and BPM-II systems. It was from the figure that the T. No. of both Na^+ ion and Cl^- ions decreased with increase in time for both the systems. This was because NaCl concentration that was available for migration started to decrease with increase in time as discussed above. However, the performance was running steadily due to the current carried by the dissociated water products of H^+ and OH^- ions. In both IEM systems the chloride ion T. No. was observed to be greater than the sodium ion T. No. as reported in literature. The initially observed higher values of T. No. of sodium (0.33) and chloride (0.54) ions decreased to 0.05–0.09, respectively, for BPM-I system. Whereas, in the case of BPM-II system, the T. No. of sodium and chloride ions decreased from their initial values of 0.4 and 0.5–0.37 and 0.42, respectively, in brine desalination performance.

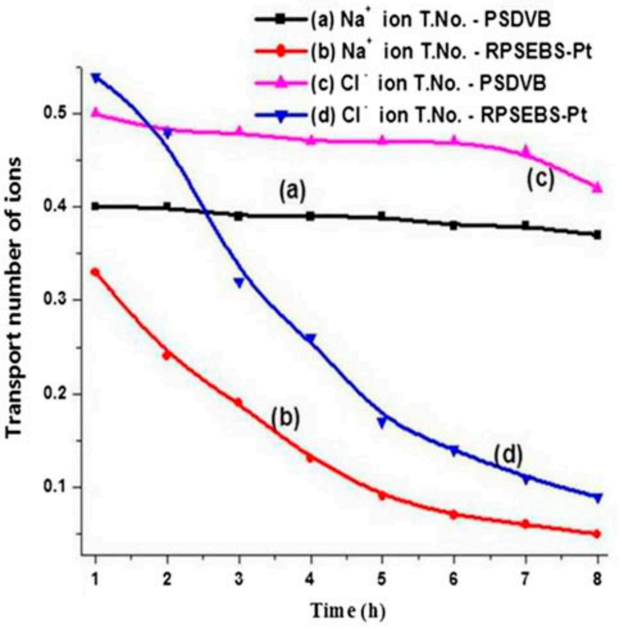

Fig. 6. Change in both sodium and chloride ions T. No. with time.

Based on feed concentration, membrane capacity and pH variation in AC and BC during the stack performance, the occurrence of water dissociation at BPM interface was confirmed. From Fig. 7, it was clear that WDE increased with increase in time. The reason for this variation of WDE with time is the same as discussed for T. No. of ions. A higher WDE of 0.86 was obtained for BPM-I and it was 0.21 for BPM-II system. The higher T. No. and steady increase in WDE with time observed for BPM-I system was due to (i) the increase in electric field, (ii) the pre-polarization of water molecules at the membrane–solution interface, and (iii) the presence of a catalytic Pt intermediate in between the two monopolar layers of BPM. It was also noted from Fig. 7 that in both cases (acidic or basic), the water dissociation fluxes decreased with time. The

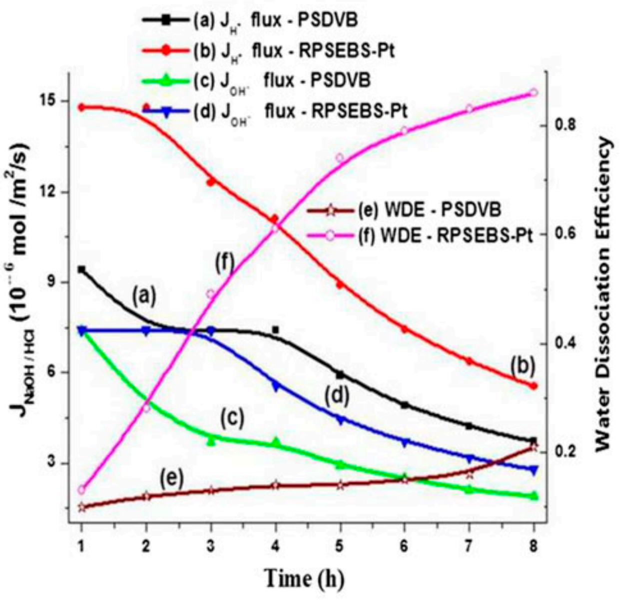

Fig. 7. Change in WDE and water dissociation fluxes of both proton and hydroxyl ion with time.

main reason for the decrease in acid and base fluxes was due to (i) the depletion of Na^+ in anode compartment and Cl^- ion in cathode compartment and (ii) the availability of NaCl in FC for the conversion into the acid and base. The highest acidic and basic fluxes observed in the present study was 9.4×10^{-6} and 7.4×10^{-6} Mol m^{-2} s^{-1} for BPM-II and 14.8×10^{-6} and 7.41×10^{-6} Mol m^{-2} s^{-1} for BPM-I systems, respectively. According to Ren et al. [29], the reduction in the ionic transport rate during later stages of the performance was often correlated with an increased membrane resistance due to the presence of a mixture of organic matter and inorganic salts. As a consequence, during the performance of brine desalination, a slight membrane fouling was observed for both BPM-I and BPM-II systems.

3.5.4. Current and voltage measurements

From Fig. 8, the current and voltage were observed to be directly proportional to each other, thereby proving that water was split at the BPM junction of BPM-I system. Also, in order to avoid high resistance, the membrane thickness used to be as thin as possible [30]. For BPM-I and BPM-II system the maximum potential point observed was 11.8–22.5 V, respectively, while the maximum current value observed for the same was 68–89 mA, respectively. The observed low voltage for BPM-I system could be explained theoretically using protonation and de-protonation reaction model and the hydrophilicity change in the interface [11].

The current variation was observed to increase with time for both BPM-I and BPM-II systems as shown in Fig. 8 due to the production of OH^-/H^+ by water dissociation. In FC, the decrease in salt concentration due to continuous ion transport resulted in higher resistance. The higher resistance observed initially in AC and BC because of lower concentrations of acid and alkali decreased due to increase in acid and base concentrations with the increase in time. The net effect of this was the overall decrease in stack resistance with time. In case of voltage versus time curve as per Fig. 8, a line parallel to *X*-axis indicated that both BPM-I and BPM-II systems were chemically stable as described by Xue et al. [31]. The purity of acid and alkali increased with an increase in voltage to some extent, after which further increase in voltage caused heating of stack which resulted in the deterioration of membrane properties.

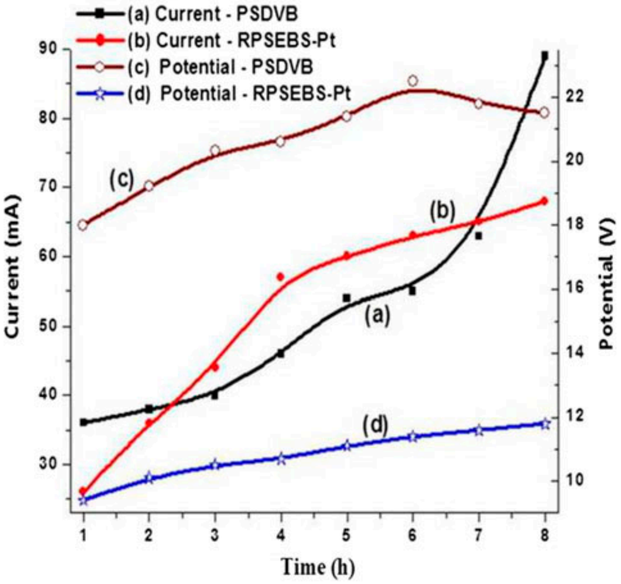

Fig. 8. Current and potential changes with time for the stack performance.

3.5.5. Determination of process efficiency parameters

For any system, higher CE with lower energy consumption is one of the factors which determine the feasibility of electrochemical process toward higher process efficiency. It is clear from Fig. 9 that CE of BPMED stack decreased with operation time for both systems. This can be explained by invoking the concept of ion leakage through IEM as discussed in T. No. of ions. CE was observed to decrease with time from 38% for BPM-II system and from 66% for BPM-I system. On the other hand, the energy consumption increased with time as shown in Fig. 9. The increase in the energy consumption was mainly attributed to the fact that a large part of the total electrical energy was consumed to overcome the electrical resistance. The decline in the applied voltage at the start of the BPMED procedure was due to either the increase in conductivity of the HCl/NaOH solution in AC/BC or due to the exhaustion of NaCl in the feed solution. The increase in resistance of FC, resulted from the exhaustion of NaCl in the solution, was offset by the decrease in electrical resistance of AC and BC caused by the increase in HCl and NaOH concentrations as a consequence of transfer of Cl^- and Na^+ ions from the feed solution. Since the transformation of NaCl into acid and base solutions was fully realized, the electrical resistance of feed solution increased, resulting in a sharp increase in the voltage drop. Thus, the energy consumption was observed to increase with time and reached a maximum of 6.2 Wh for BPM-II and 6.41 Wh for BPM-I systems.

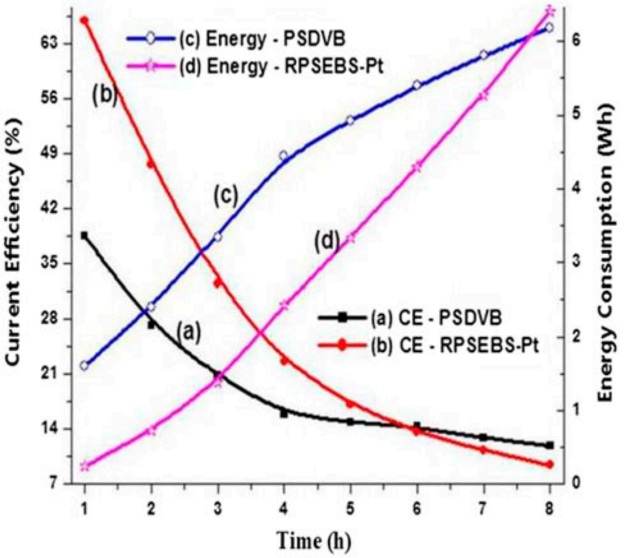

Fig. 9. Change in CE and energy consumption with time for the stack performance.

3.5.6. Determination of salinity in feed solution

To evaluate the purity of the generated acid and base and to confirm the BPM's capacity to dissociate water, salinity of FC solution was analyzed for both BPM-I and BPM-II systems. The effectiveness in removing NaCl ions from the FC was confirmed by its salinity measurements. The observance of lower salinity (of about 5.2–7.9% in the case of BPM-I and BPM-II systems, respectively) than their initial values (of about 11.5% for both the systems) was mainly because of the migration of the salt ions under the electric field from the FC toward the neighboring compartments. Thus, this result suggested that the water obtained after the BPMED desalination process was of better quality than the initial sample. The higher the difference between the initial and final values indicated the process effectiveness in the removal of NaCl and higher acid–base production.

4. Conclusion

Resin–glass fiber-reinforced and -functionalized PSEBS IEMs were prepared and characterized using TGA and contact angle measurements. The chemical stability of the prepared IEMs was evaluated by means of ionic conductivity, water absorption, and IEC. The BPM efficiency of BPM-I and BPM-II based systems were evaluated using pH and concentration measurements. Brine desalination performance was analyzed for both BPM-I- and BPM-II-based systems and compared. Based on the results obtained for CE (66% for BPM-I and 38% for BPM-II), the lowest energy consumption (0.24 Wh for BPM-I and 1.6 Wh for BPM-II), acid–base production (0.012 N acid and 0.006 N base for BPM-I and 0.008 N acid and 0.004 N base for BPM-II), and WDE (0.86 for BPM-I and 0.21 for BPM-II), it was concluded that BPM-I system showed a better performance than that of the commercial BPM-II-based IEM system.

Supplementary material

The supplementary material for this paper is available online at http://dx.doi.10.1080/19443994.2016.1165737.

Acknowledgment

Financial support from the Board of Research in Nuclear Science (BRNS), Mumbai, India (Letter No. 2010/37C/1/BRNS/826, Dated: 28-06-2010) is gratefully acknowledged. The authors thank for Goniometer facility help in Polymer Engineering and Colloids Science Laboratory, Chemical Engineering Department, IIT Madras.

Abbreviation list

AC — acid compartment
AEL — anion-exchange layer
AEM — anion-exchange membrane
AER — anion-exchange resin
BC — base compartment
BPM — bipolar membrane
BPMED — bipolar membrane electrodialysis
BVA — bovine serum albumin
CE — current efficiency
CEL — cation-exchange layer
CEM — cation-exchange membrane
CER — cation-exchange resin
Cl^- — chloride ion
EC — electrolyte compartment
ED — electrodialysis
FC — feed compartment
HCl — hydrochloric acid
H_3O^+ — hydronium ion
OH^- — hydroxyl ion
IEC — ion-exchange capacity
IEL — ion-exchange layers
IEM — ion-exchange membrane
IER — ion-exchange resin
IL — intermediate layer
PSEBS — poly(styrene–ethylene–butylene–polystyrene)

NaCl — sodium chloride
PAMAM — polyamido amine
PEG — polyethylene glycol
PSDVB — polystyrene–divinylbenzene
PVA — polyvinyl alcohol
Pt — platinum
H^+ — proton
QPSEBS — quaternized poly(styrene–ethylene–butylene–polystyrene)
RAEM — reinforced anion-exchange membrane
RBPM — reinforced bipolar membrane
BPM-I — RPSEBS-Pt IEM system
BPM-II — PSDVB IEM system
RO — reverse osmosis
RCEM — reinforced cation-exchange membrane
RQPSEBS — reinforced quaternized poly(styrene–ethylene–butylene–polystyrene)
RSPSEBS — reinforced sulfonated poly(styrene–ethylene–butylene–polystyrene)
Na^+ — sodium ion
NaOH — sodium hydroxide
SPSEBS — sulfonated poly(styrene–ethylene–butylene–polystyrene)
THF — tetrahydrofuran
T. No. — transport number
WDE — water dissociation efficiency

References

[1] H.K. Lonsdale, The growth of membrane technology, J. Membr. Sci. 10 (1982) 81–181.

[2] V.V. Volkov, B.V. Mchedlishvili, V.I. Roldugin, S.S. Ivanchev, A.B. Yaroslavtsev, Membranes and nanotechnologies, Nanotechnol. Russ. 3 (2008) 656–687.

[3] O. Kuroda, O.S. Takahashi, S. Kubota, K. Kikuchi, Y. Eguchi, Y. Ikenaga, N. Sohma, K. Nishinoiri, S. Wakamatsu, S. Itoh, An electrodialysis sea water desalination system powered by photovoltaic cells, Desalination 67 (1987) 33–41.

[4] S.S. Ivanchev, Fluorinated proton-conduction nafion-type membranes, the past and the future, Russ. J. Appl. Chem. 81 (2008) 529–545.

[5] N.V. Sheldeshov, N.P. Gnusin, V.I. Zabolotskii, N.D. Pis'menskaya, Chronopotentiometric study of electrolyte transport in commercial bipolar membranes, Soviet, Electrochemistry 22 (1987) 742–750.

[6] Y. Tanaka, S. Matsuda, Y. Sato, M. Seno, Concentration polarization and dissociation of water in ion exchange membrane electrodialysis, the effects of electrolytes on the dissociation of water, J. Electrochem. Soc. Jpn. 50 (1982) 667–672.

[7] M.S. Kang, Y.J. Choi, H.J. Lee, S.H. Moon, Effects of inorganic substances on water splitting in ion-exchange membranes I: Electrochemical characteristics of ion-exchange membranes coated with iron hydroxide/oxide and silica sol, J. Colloid Interface Sci. 273 (2004) 523–532.

[8] M.S. Kang, Y.J. Choi, S.H. Moon, Effects of inorganic substances on water splitting in ion-exchange membranes II: Optimal contents of inorganic substances in preparing bipolar membranes, J. Colloid Interface Sci. 273 (2004) 533–539.

[9] F. Hanada, K. Hirayama, S. Tanaka, N. Ohmura, Bipolar membrane and method for its production, JP Patent 2524012 (1996).

[10] F.G. Wilhelm, N.F.A. vander vegt, M. Wessling, H. Strathmann, Bipolar membrane preparation, in: A.J.B. Kemperman (Ed.), Bipolar Membrane Handbook, Twente University Press, Enschede, The Netherlands, 2000, pp. 79–108.

[11] R.Q. Fu, T.W. Xu, G. Wang, W.H. Yang, Z.X. Pan, PEG–catalytic water splitting in the interface of a bipolar membrane, J. Colloid Interface Sci. 263 (2003) 386–390.

[12] R.Q. Fu, Y.H. Xue, T.W. Xu, W.H. Yang, Fundamental studies on the intermediate layer of a bipolar membrane Part IV. Effect of polyvinyl alcohol (PVA) on water dissociation at the interface of a bipolar membrane, J. Colloid Interface Sci. 285 (2005) 281–287.

[13] R.Q. Fu, T.W. Xu, W.H. Yang, Z.X. Pan, Fundamental studies on the intermediate layer of a bipolar membrane Part II. Effect of bovine serum albumin (BSA) on water dissociation at the interface of a bipolar membrane, J. Colloid Interface Sci. 278 (2004) 318–324.

[14] R.Q. Fu, T.W. Xu, Y.Y. Cheng, W.H. Yang, Z.X. Pan, Fundamental studies on the intermediate layer of a bipolar membranePart III. Effect of starburst dendrimer PAMAM on water dissociation at the interface of a bipolar membrane, J. Membr. Sci. 240 (2004) 141–147.

[15] B. Bauer, F.J. Gerner, H. Strathmann, Development of bipolar membranes, Desalination 68 (1988) 279–292.

[16] K. Venugopal, S. Dharmalingam, Fundamental studies on a new series of SPSEBS-PVA-QPSEBS bipolar membrane: Membrane preparation and characterization, J. Appl. Polym. Sci. 127 (2013) 4983–4990.

[17] M. Kumar, V.K. Shahi, Heterogeneous–homogeneous composite bipolar membrane for the conversion of salt of homologous carboxylates into their corresponding acids and bases, J. Membr. Sci. 349 (2010) 130–137.

[18] K. Venugopal, S. Dharmalingam, Electrodialysis desalination of brine water with simultaneous recovery of acid and base, Int. J. Emerging Trends Electr. Electron. 11 (2015) 108–119.

[19] K. Venugopal, S. Dharmalingam, Desalination efficiency of a novel bipolar membrane based on functionalized polysulfone, Desalination 296 (2012) 37–45.

[20] K. Venugopal, S. Dharmalingam, Evaluation of synthetic salt water desalination by using a functionalized polysulfone based bipolar membrane electrodialysis cell, Desalination 344 (2014) 189–197.

[21] K. Venugopal, S. Dharmalingam, Investigation on the application of polysulfone based bipolar membrane for desalination of water, Desalin. Water Treat. 54 (2015) 285–294.

[22] C.R. Dias, M.N. de Pinho, Water structure and selective permeation of cellulose-based membranes, J. Mol. Liq. 80 (1999) 117–132.

[23] R. Guan, H. Zou, D. Lu, C. Gong, Y. Liu, Polyethersulfone sulfonated by chlorosulfonic acid and its membrane characteristics, Eur. Polym. J. 41 (2005) 1554–1560.

[24] S. Sachdeva, R.P. Ram, J.K. Singh, A. Kumar, Synthesis of anion exchange polystyrene membranes for the

electrolysis of sodium chloride, AIChE J. 54 (2008) 940–949.

[25] X. Zhu, Y. Liang, H. Pan, X. Jian, Y. Zhang, Synthesis and properties of novel H-bonded composite membranes from sulfonated poly(phthalazinone ether)s for PEMFC, J. Membr. Sci. 312 (2008) 59–65.

[26] J. Shen, J. Huang, L. Liu, W. Ye, J. Lin, B.V. Bruggen, The use of BMED for glyphosate recovery from glyphosate neutralization liquor in view of zero discharge, J. Hazard. Mater. 260 (2013) 660–667.

[27] Y. Wang, X. Zhang, C. Huang, T. Xu, Production of monoprotic, diprotic, and triprotic organic acids by using electrodialysis with bipolar membranes: Effect of cell configurations, J. Membr. Sci. 385–386 (2011) 226–233.

[28] T. Xu, W. Yang, Effect of cell configurations on the performance of citric acid production by a bipolar membrane electrodialysis, J. Membr. Sci. 224 (2002) 1–9.

[29] H. Ren, Q. Wang, X. Zhang, R. Kang, S. Shi, W. Cong, Membrane fouling caused by amino acid and calcium during bipolar membrane electrodialysis, J. Chem. Technol. Biotechnol. 83 (2008) 1551–1557.

[30] J. Balster, S. Srinkantharajah, R. Sumbharaju, I. Pünt, R.G.H. Lammertink, D.F. Stamatialis, M. Wessling, Tailoring the interface layer of the bipolar membrane, J. Membr. Sci. 365 (2010) 389–398.

[31] Y.H. Xue, R.Q. Fu, Y.X. Fu, T.W. Xu, Fundamental studies on the intermediate layer of a bipolar membrane V. Effect of silver halide and its dope in gelatin on water dissociation at the interface of a bipolar membrane, J. Colloid Interface Sci. 298 (2006) 313–320.